Optimal Decreased Torque Gain Control for Maximizing Wind Energy Extraction Under Varying Wind Speed

Liansong Guo, Minghui Yin, Chenxiao Cai, Yunyun Xie, and Yun Zou

Abstract—**Optimal torque (OT) control is a widely used method for maximum power point tracking (MPPT) due to its simplicity. In order to overcome the adverse impacts of turbulent wind speed variations on MPPT, in several methods, modification factors have been proposed to dynamically modify the ideal power curve for OT control. However, this paper finds that the update cycles used in existing methods to adjust power curve modification factors are very long and hence these factors are difficult to be updated in a timely manner along with the wind speed variations. This thereby may deteriorate the effectiveness of wind energy extraction. Therefore, an optimal decreased torque gain (DTG) control method is proposed in this paper. Based on the persistence method, an offline mapping from the wind speed and rotor speed to optimal modification factors is established via optimal control theory. The power curve can be periodically modified online through the mapping relationship. In this method, the update cycles for these power curve modification factors are shortened from tens of minutes to seconds. The simulations and experiments show that the proposed method is more efficient than others in terms of energy extraction under varying wind speeds, especially for turbulent wind cases.**

Index Terms—**Decreased torque gain (DTG), maximum power point tracking (MPPT), offline mapping, optimal control, persistence method.**

I. INTRODUCTION

WIND power generation has developed rapidly in recent years, and it offers prospects for the exploitation of clean energy resources. The improvements in wind energy extraction efficiency have received increasing attention. In this field, maximum power point tracking (MPPT) control is widely implemented in variable-speed wind turbines (VSWTs) [1]-[4]. Optimal torque (OT) control is the most widely used engineering method in MPPT strategies.

The OT control is designed based on the theoretically optimal power curve and aims to keep the rotor running at the maximum power point (MPP). Due to sluggish dynamics, a wind turbine is difficult to accelerate or decelerate quickly to respond to wind variations under OT control [5]-[7]. In this case, the rotor cannot work at the MPP, which seriously reduces the effectiveness of wind energy extraction.

To address this issue, several methods have been proposed to modify the optimal power curve. These methods can be roughly summarized as the following three types.

1) Decreased torque gain (DTG) [5] and adaptive torque control (ATC) [8]-[11] methods. A proportionality coefficient of the optimal power curve is added to decrease the torque of the generator.

2) Inertia compensation control (ICC) [12] and constant bandwidth control (CBC) [13] methods. A compensation term for the generator torque is added to increase the torque discrepancy.

3) Reduction of tracking range (RTR) [14], [15] and effective tracking range (ETR) [16] methods. The defined range of the optimal power curve is reduced to shorten the tracking distance required for MPPT.

In these methods, the theoretically optimal power curve is modified through different modification factors to speed up the MPPT process. The sluggish dynamics of wind turbines, which cause a reduction in wind energy extraction efficiency, can be mitigated to some extent. Generally, the values of the optimal modification factors vary with the observed wind conditions [5]. To adapt to varing wind speeds, these modification factors should be dynamically adjusted to improve the effectiveness of wind energy extraction.

However, it is found that the update cycles for power curve modification factors are too long to adapt to varying wind speeds. The update cycles in these existing methods are generally within 10-20 min [10], [17]. In contrast, turbulent wind speeds often fluctuate drastically within seconds. The modification factors are difficult to adapt to these wind speeds due to their long update cycles. This impedes the further capture of wind energy.

In this paper, an optimal DTG control strategy is proposed. To obtain the optimal modification factors under varying wind speeds, the persistence method [18]-[22] is applied. It treats the wind speed in a very short time horizon as a constant value. Hence, an offline mapping from the wind speed and rotor speed to optimal modification factors can be

Manuscript received: May 6, 2021; revised: November 2, 2021; accepted: February 2, 2022. Date of CrossCheck: February 2, 2022. Date of online publication: March 29, 2022.

This work was supported by the National Natural Science Foundation of China (No. 61773214).

L. Guo, M. Yin, C. Cai, Y. Xie, and Y. Zou (corresponding author) are with the School of Automation, Nanjing University of Science and Technology, Nanjing 210094, China (e-mail: liansguo@126. com; ymhui@vip. 163. com; ccx5281@njust.edu.cn; yunyun_xie@njust.edu.cn; zouyun@njust.edu.cn).

DOI: 10.35833/MPCE.2021.000274

established based on optimal control theory. According to this mapping relationship, at the beginning of each cycle, the optimal modification factors can be adjusted by estimating the wind speed and measuring the rotor speed in real time. The optimal control command determined by the optimal modification factors can be updated to cope with varying wind speeds in a shorter cycle. The effectiveness of wind energy extraction under turbulence is thus enhanced. The major contributions of this paper are summarized as follows.

1) It is found that the update cycles for the power curve modification factors should be shortened to adapt to varying wind speeds. The update cycles of the modification factor in existing methods generally last for 10-20 min. They are difficult to adapt to wind speeds that vary within seconds. This impedes the further improvement of wind energy extraction.

2) A new method for periodically updating power curve modification factors is proposed based on optimal control theory. An offline mapping from the wind speed and rotor speed to power curve modification factors is established. The control command is updated in a shorter cycle. The method thereby adapts better to varying wind speeds.

The remainder of this paper is organized as follows. Section II introduces wind turbine modeling and a review of the OT control. In Section III, an optimal control method for maximizing wind energy extraction efficiency by adjusting the MPPT control command factors with shorter updating cycles is presented. In Section IV, simulations based on the fatigue, aerodynamics, structures, and turbulence (FAST) [23] code and experiments conducted on a wind turbine simulator (WTS) [24] demonstrate the effectiveness of the proposed method. Finally, Section V concludes this paper.

II. Wind Turbine Modeling and a Review of OT Control

In this section, the modeling process for a VSWT with OT control is introduced. Several methods have been developed to further improve the effectiveness of wind energy extraction. It is discovered that the update cycles of power curve modification factors with the corresponding controllers employed in these methods are difficult to adapt to varying wind speeds. Therefore, it is urgently necessary to propose a new method to shorten these cycles to maximize the extracted wind energy.

A. Modeling of a VSWT with OT Control

The aerodynamic power extracted from the wind by a VSWT is [1]-[7]:

$$P_r = 0.5\rho\pi R^2 v^3 C_p(\lambda) \tag{1}$$

where ρ is the air density; R is the rotor radius; v is the wind speed; and C_p is a function of the tip speed ratio (TSR) λ, which is expressed as:

$$\lambda = \frac{\omega_r R}{v} \tag{2}$$

where ω_r is the rotor speed. For a given period, the captured wind energy E is the integral of the power, which can be expressed as:

$$E = \int P_r \mathrm{d}t = \int 0.5\rho\pi R^2 v^3 C_p \mathrm{d}t \tag{3}$$

The aerodynamic torque T_r is then given by:

$$T_r = P_r / \omega_r \tag{4}$$

The mechanical characteristics of a wind turbine can be described for a two-mass model, which is expressed as [16]:

$$\begin{cases} J_r\dot{\omega}_r + D_r\omega_r = T_r - T_{ls} \\ J_g\dot{\omega}_g + D_g\omega_g = T_{hs} - T_e \\ T_{hs} = T_{ls}/n_g \end{cases} \tag{5}$$

where T_e is the electromagnetic torque of the generator; J_r and J_g are the inertia values of the wind wheel and generator, respectively; D_r and D_g are the external dampings of the rotor and generator, respectively; T_{ls} and T_{hs} are the low-speed and high-speed shaft torque values, respectively; n_g is the gear ratio of the gearbox; and ω_g is the generator speed. Assuming a perfectly rigid shaft and ignoring the damping coefficients, the mechanical dynamics can be simplified to a single lumped-mass model:

$$\dot{\omega}_r = (T_r(v, \omega_r) - T_g)/J_t \tag{6}$$

where $J_t = J_r + n_g^2 J_g$; and $T_g = n_g T_e$, T_g is regarded as the control command. When a VSWT runs at the optimal TSR value λ_{opt} all the time, the power coefficient C_p remains at its maximal value (denoted as C_p^{max}), as shown in Fig. 1. Then, the captured wind energy reaches its maximal value, which is expressed as:

$$E_{max} = \int P_r^{max} \mathrm{d}t = \int 0.5\rho\pi R^2 v^3 C_p^{max} \mathrm{d}t \tag{7}$$

The wind energy extraction efficiency is expressed as:

$$\eta = E/E_{max} \tag{8}$$

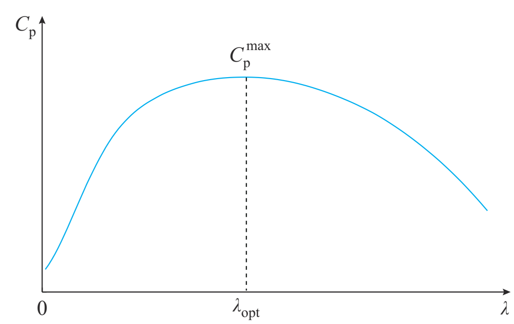

Fig. 1. Typical $C_p(\lambda)$ curve.

The control strategy based on the traditional OT control can be expressed as [7]:

$$T_g = K_{opt}\omega_r^2 \tag{9}$$

$$K_{opt} = (0.5\rho\pi R^5 C_P^{max})/\lambda_{opt}^3 \tag{10}$$

where K_{opt} is the theoretically OT gain derived from the theoretically optimal power curve. When a VSWT operates according to the ideal optimal curve, the extracted wind energy is E_{max}. However, due to rapid wind speed fluctuations, the operation power points stray from the maximum continuously with the slow dynamics of the VSWT. This results in reduced wind energy extraction.

B. Review of OT Control

Noting that more wind energy is contained in wind gusts than in wind lulls [5], [16], three mainstream methods have been introduced to accelerate the tracking of wind gusts.

1) DTG Method

The generator torque of a DTG controller is given by:

$$T_g = \alpha K_{opt} \omega_r^2 \tag{11}$$

where $\alpha \in [0, 1]$ is the DTG modification factor. The unbalanced torque discrepancy of the turbine increases as the generator torque decreases. This thereby accelerates the process for tracking wind gusts.

For variable wind speeds in a given period, there exists a unique α corresponding to the maximum extracted wind energy [5]. Nevertheless, only a rough interval estimation of α is provided via DTG control [5]. Thus, to enhance wind energy extraction, ATC methods [8]-[11] have been further developed to dynamically adjust α depending on time-varying wind conditions.

2) ICC Method

The generator torque of an ICC controller is given by:

$$T_g = K_{opt} \omega_r^2 - k_f \dot{\omega}_r \tag{12}$$

where k_f is the compensation factor [12], [13]. As in the DTG method, the unbalanced torque discrepancy of the turbine increases to accelerate the MPPT process. As the decrease in torque is proportional to the rotor acceleration, a dramatic torque variation is observed. k_f should be selected carefully so that the drive train load can be cut down in this method [5], [25].

3) RTR Method

Unlike the methods that decrease the generator torque, the RTR method focuses on shortening the tracking distance to increase the acceleration of turbines with increasing wind speeds. The implementation involves constraining the starting speed so that a higher rotor speed will be achieved more quickly as the wind speed increases [14], [15].

To periodically update the starting speed, the ETR method [16] was proposed to establish a direct quantitative relationship between the reduction in the tracking range and the observed wind conditions.

C. Deficiency of Update Cycles for Modified Factors

There exists a serious defect in these existing methods that the update cycles of the corresponding modification factors generally spend 10-20 min. In contrast, wind speeds vary within seconds. It is difficult for a factor that is kept constant over a relatively long period to adapt to varying wind speeds with high accuracy. Thus, this cannot improve the wind energy extraction.

Taking the DTG method as an example, an analysis is provided. The power curve modification factor in the DTG method is the torque gain α. Under a turbulent wind speed, the optimal α for achieving maximum wind energy extraction over 10 min and 10 s is simulated, as shown in Fig. 2. The optimal α fluctuates more frequently in a shorter period, which also improves the wind energy extraction by approximately 1.5%. This means that a shorter period of adjusting α can be used to better adapt to varying wind speeds. The wind energy extraction efficiency can be further improved.

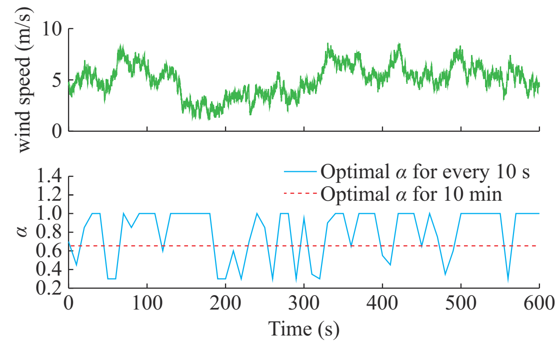

Fig. 2. Optimal α in different update cycles.

Therefore, a new method for shortening these cycles is urgently required to further improve the wind energy extraction efficiency.

III. Optimal Control Method for Maximizing Wind Energy Extraction Efficiency

In this section, a method is proposed by means of optimal control theory. In this method, an offline mapping from the rotor speed and wind speed to optimal modification factors in an integrated controller is established. The modification factors are updated periodically according to the mapping relationship. The cycles can be significantly shortened, and the wind energy extraction results can be further enhanced.

A. Design of Integrated Controller

In order to improve the acceleration ability of the single DTG method with respect to tracking wind lulls, an integrated controller is designed by adding an ICC compensation term to the DTG controller.

The electromagnetic torque, as a control input command, can be expressed as:

$$T_g = \alpha K_{opt} \omega_r^2 - \zeta \tag{13}$$

where ζ is developed from the ICC method; and $\alpha \in [0, 1]$ is developed from the DTG. Both parameters are regarded as power curve modification factors. The optimal and modified power curves are shown in Fig. 3, where v_1-v_5 are different wind speeds.

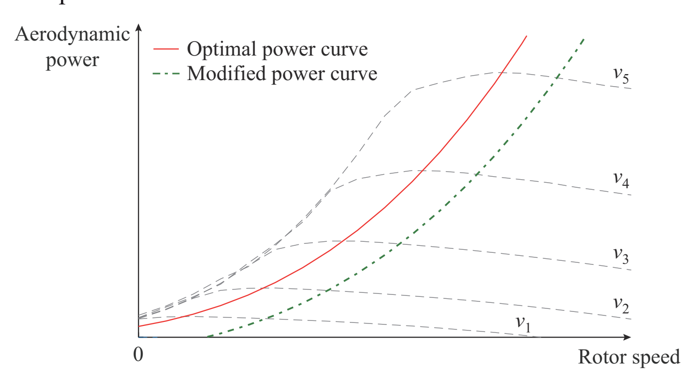

Fig. 3. Optimal and modified power curves.

Compared with that of the DTG method, the tracking ability for wind lulls of the proposed method is strengthened with an additional decreased torque factor ζ. Similarly, as ζ is not dependent on the rotor speed, the dramatic variability in the torque demand can also be mitigated relative to that of the ICC method. In summary, the integrated controller remedies the deficiencies of the individual controllers.

In the proposed method, two modification factors must be optimized. Most of the previous improvements such as the ATC scheme developed for the DTG are only applicable to dynamically optimize a single factor. Therefore, a new method must be proposed. If the two modification factors can be dynamically adjusted, the original DTG method and other controllers with specific factors can also be optimized through the designed method. This indirectly demonstrates the superior ability of the proposed method.

Remark 1: the theoretically optimal power curve is obtained on the basis of the design in steady state; therefore, the offset of the equilibrium points will occur when the power curve is modified. It is thus necessary to illustrate the stability of the turbine with the modified power curve. Similar to the proof of the stability of adaptive DTG control with a single α in [8], a theorem for the stability of a wind turbine system with control law (13) is given in Appendix A.

B. Implementation of Optimal Control Method

Let T be the update cycle for the modification factors in (13). For each control time window $[kT, (k+1)T), k \in \mathbb{N}$, the modification factors α_k and ζ_k are given to update the control command. It is necessary to compute the optimal α_k^* and ζ_k^* to maximize the extracted wind energy for each cycle, as shown in Fig. 4.

Fig. 4. Optimal DTG modification factors for various control time windows.

Let τ be the length of a wind speed prediction time window. Then, the previewed wind speed in a prediction time window $[kT, kT+\tau)$ can be expressed as $v_k(t)$. The wind energy extraction in $[kT, kT+\tau)$ can be expressed as:

$$E_k(\alpha_k, \zeta_k, v_k(t), \omega_r(t)) = \int_0^\tau 0.5\rho\pi R^2 v_k^3(t) C_p(\omega_r(t), v_k(t))\mathrm{d}t \quad (14)$$

Hence, for a given $v_k(t)$, the corresponding $\alpha_k^*(v_k(t))$ and $\zeta_k^*(v_k(t))$ can be computed by solving the objective function, which is denoted as:

$$obj = \max_{\alpha_k, \zeta_k} E_k(\alpha_k, \zeta_k, v_k(t), \omega_r(t)) \quad (15)$$

s.t.

$$\begin{cases} \alpha_k \in [0, 1] \\ \zeta_k \in M \\ \omega_r(0) = \omega_r(kT) \end{cases} \quad (16)$$

where $\omega_r(kT)$ is the measured rotor speed at kT; and M is a set of numbers based on experience [5]. Hence, the optimal α_k^* and ζ_k^* for the prospective maximum extracted wind energy under the given wind speed $v_k(t)$ in $[kT, kT+\tau)$ can be obtained by:

$$\begin{cases} \alpha_k^* = \alpha_k^*(v_k(t)) \\ \zeta_k^* = \zeta_k^*(v_k(t)) \end{cases} \quad (17)$$

Based on the above assumption, the process for computing the optimal control command in a cycle under given wind speeds can be summarized as Algorithm 1.

Algorithm 1: process for computing optimal control command in a cycle under given wind speeds

1: For a given $v_k(t)$, compute the optimal α_k^* and ζ_k^* through (14)-(16) by means of the appropriate optimal control algorithm
2: Obtain the optimal control command $T_{g,k} = \alpha_k^* K_{opt}\omega_r^2 - \zeta_k^*$

In Algorithm 1, $v_k(t)$ must be given for $[kT, kT+\tau)$. However, the wind speed $v_k(t)$ is highly unpredictable in practice, and the forecasting of precise turbulent wind speeds is very difficult in a very short-term period τ due to technical limitations [26], [27]. Previously, relatively accurate wind speeds in real time could be estimated via the methods in [28], [29], as shown in Fig. 5 [28].

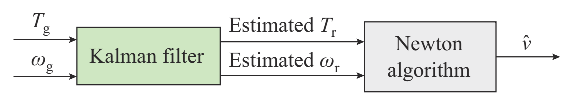

Fig. 5. Wind speed estimation.

Hence, for practical feasibility, the estimated wind speed $\hat{v}$ can be used to approximate a wind speed prediction in a very short-term period through the persistence method [21], [22]. In the persistence method, it is assumed that $v_k(t) = v(kT)$ for $[kT, kT+\tau)$. Then, from Algorithm 1, the optimal α_k^* and ζ_k^* for $[kT, kT+\tau)$ can be denoted as:

$$\begin{cases} \alpha_k^* = \alpha_k^*(v(kT), \omega_r(kT)) \\ \zeta_k^* = \zeta_k^*(v(kT), \omega_r(kT)) \end{cases} \quad (18)$$

Note that $v_k(t) = v(kT)$ in $[kT, kT+\tau)$. Due to this condition, arbitrarily variable wind speeds can be expressed as a corresponding constant. Hence, for different wind and rotor speed values $v(kT)$ and $\omega_r(kT)$, α_k^* and ζ_k^* can be computed, respectively.

Furthermore, let the ranges of possible variable wind speeds $[v_m, v_M]$ and rotor speeds $[\omega_{rm}, \omega_{rM}]$ be quantized as $V_1, V_2, ..., V_N \in [v_m, v_M]$ and $\Omega_{r1}, \Omega_{r2}, ..., \Omega_{rP} \in [\omega_{rm}, \omega_{rM}]$, where $V_1 = v_m$, $V_N = v_M$, $\Omega_{r1} = \omega_{rm}$, and $\Omega_{rP} = \omega_{rM}$. Then, for all $V_n \in \{V_1, V_2, ..., V_N\}$ and all rotor speeds $\Omega_{rn} \in [\Omega_{r1}, \Omega_{rP}]$, the corresponding optimal modification factors $\alpha^*(V_n, \Omega_{rn})$ and $\zeta^*(V_n, \Omega_{rn})$ can be computed in advance through Algorithm 1. In other words, an offline mapping from the rotor speed and wind speed to modification factors can be established:

$$(\alpha^*, \zeta^*) = f_{\alpha,\zeta}(V_n, \Omega_{rn}) \quad 1 \le n \le N \quad (19)$$

where $f_{\alpha,\zeta}$ is the mapping relationship. At the start time of each cycle, the optimal modification factors can be mapped through the estimation of the wind speed and the measurement of the rotor speed.

The designed control strategy, as shown in Fig. 6, can be summarized in Algorithm 2.

From the design procedure utilized for the optimal controller, a shortened update cycle is adopted by the proposed method.

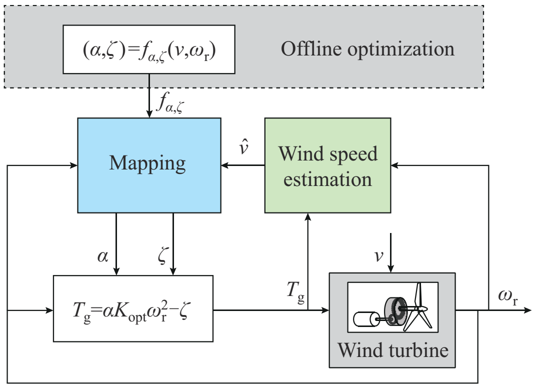

Fig. 6. Scheme of designed control strategy.

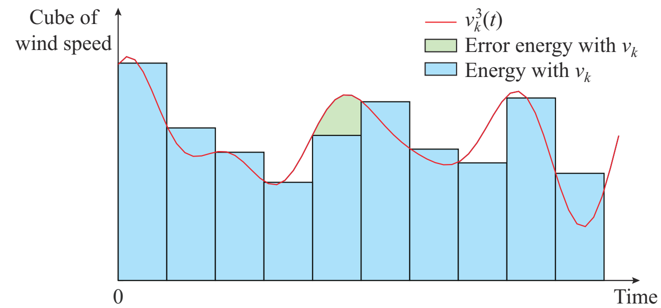

Fig. 7. Distribution of error energy with persistence method.

Algorithm 2: process for computing optimal control command in a cycle under unknown wind speeds

1: Obtain $f_{\alpha,\zeta}$ by computing $\alpha^*(V_n, \Omega_{rn})$ and $\zeta^*(V_n, \Omega_{rn})$ for all V_1, and $\Omega_{r1}, \Omega_{r2}, \ldots, \Omega_{rP} \in [\omega_{rm}, \omega_{rM}]$ offline

2: Estimate the wind speed $v(kT)$ and measure the rotor speed $\omega_r(kT)$ at kT online, and quantize them to V_{n_k} and Ω_{n_k}, $1 \le n_k \le N$, $k \in \mathbb{N}$

3: Set $(\alpha_k^*, \zeta_k^*) = f_{\alpha,\zeta}(V_{n_k}, \Omega_{r,n_k})$ and update $T_{g,k}^* = \alpha_k^* K_{opt}\omega_r^2 - \zeta_k^*$ for $[kT, (k+1)T)$ in real time

Remark 2: in this paper, the GPOPS-II algorithm [30]-[32] based on the Gaussian pseudospectral method is used to solve the optimal α_k^* and ζ_k^* values in Algorithms 1 and 2. It was developed from the Pontryagin maximum principle, which has been found to be an efficient tool for solving general continuous-time optimal control problems. More details are given in Appendix B.

Remark 3: in Algorithm 2, the wind speed function $v_k(t)$ is replaced by a constant V_n in $[kT, kT+\tau)$. The effect of the resulting error can be estimated as follows.

Suppose $v_k(t)$ is replaced by V_n in $[kT, kT+\tau)$. By the generalization of the first integral intermediate value theorem, there exists a variable v_ξ that makes (20) valid.

$$v_\xi^3 \int_0^\tau C_p(\lambda)\mathrm{d}t = \int_0^\tau v_k^3(t) C_p(\lambda)\mathrm{d}t \tag{20}$$

where $v_\xi \in [v_m, v_M]$. Since $C_p \ll v_k^3(t)$, the error occupation proportion of the energy can be described by:

$$\Delta\varepsilon = \left| \frac{(v_\xi^3 - V_n^3)\Delta t}{\int_0^\tau v_k^3(t)\,\mathrm{d}t} \right| \tag{21}$$

where $\Delta\varepsilon$ is the loss rate of wind energy with the persistence estimation. As shown in Fig. 7, the value of this error relies on the selection of T and τ.

IV. Simulation and Analysis

To verify the method proposed in this paper, FAST-based simulations and WTS-based experiments on a three-bladed controls advanced research turbine (CART3) [23] built by the National Renewable Energy Laboratory (NREL) are used. The parameters of the wind turbine are shown in Table I.

TABLE I
Parameters of Wind Turbine

Parameter	Value
Number of blades	3
Rotor radius	20 m
Hub height	36.6 m
Rated power	600 kW
Gearbox ratio	43.165
Rated torque	3580 N·m
λ_{opt}	5.8
C_p^{max}	0.46

As the persistent wind speed is applied to replace the forecasted wind speed in $[kT, kT+\tau)$, the length τ directly affects the optimization calculation error. The accurate wind speed $v_k(t)$ cannot be approximated by V_n if the value of τ is too large. In contrast, a narrow range of the control update period $[kT, (k+1)T)$ may lead to a frequent response to the control commands of wind turbines.

Thus, the dynamic response time interval of the wind power control system is investigated. According to the time required for returning to the steady state after the disturbance, we choose $\tau = 10$ s. To better respond to varying wind speeds, we choose $T = 8$ s.

A. Performance Comparison Using FAST Simulation

In addition to the results of wind energy extraction, the evaluation results for the error according to the persistence method are discussed to estimate the prospective wind speed.

1) Estimation of Wind Energy Loss Caused by Persistence Method

As the varying wind speeds are replaced by a constant value in the calculation, the resulting loss of wind energy capture efficiency needs to be estimated. The $\Delta\varepsilon$ value in each control cycle is plotted in Fig. 8.

As shown in Fig. 8, the energy error proportion in each control cycle is much smaller. In fact, the values are determined by the selection of the values of τ and T. The calculation error obtained by the persistence method decreases with the length of the prediction time window $[kT, kT+\tau)$.

The comparison of rotor speed trajectories with persistence method and segmental prediction hypothesis is shown in Fig. 9, where ω_{opt} represents the ideal rotor speed.

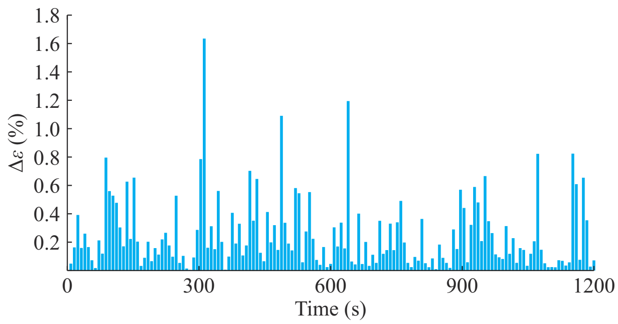

Fig. 8. Δε in each control cycle.

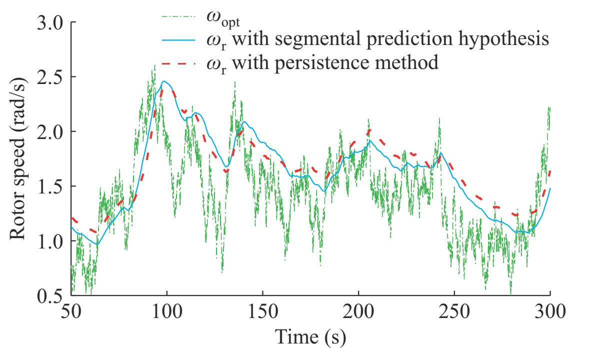

Fig. 9. Comparison of rotor speed trajectories with persistence method and segmental prediction hypothesis.

The segmental prediction hypothesis supposes that the wind speed in each interval $[kT, kT+\tau)$ can be accurately predicted. With this assumption, the optimal commands are obtained through Algorithms 1 and 2, respectively. Their wind energy extraction efficiencies, which are 91.43% and 91.35%, respectively, confirm that the chosen prediction horizon and control cycle are reasonable. This result reflects the slight effect on the wind energy extraction efficiency in each prediction time window with the persistence method.

2) Comparisons of Wind Energy Extraction Efficiency

Next, to compare the wind energy extraction effect, the applications of optimizing the DTG modification factor by means of the proposed method and by the ATC method are added. As the iteration cycle of ATC is much longer, the total simulation time is set to be 1 hour. The cycle of ATC is set to be 10 min. A signal of turbulent wind speed with an average speed of 4 m/s and a high level of turbulence intensity are applied as the input of the wind turbine.

The comparison of η for different methods using FAST simulation is shown in Fig. 10. The comparison of α for different methods using FAST simulation is shown in Fig. 11. For a clear comparison, the factor ζ is normalized to the range of [0, 1]. The modification factors in the proposed method are better adapted to varying wind speeds. This thereby enhances the wind energy extraction efficiency in each cycle.

As can be observed in Fig. 12, the operation rotor speeds for the proposed method and ATC are almost higher than that of the conventional OT control. More energy is captured in wind gusts, which is an effect of the decreased torque gain.

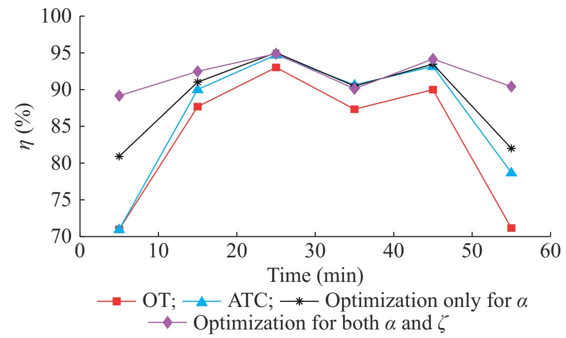

Fig. 10. Comparison of η for different methods using FAST simulation.

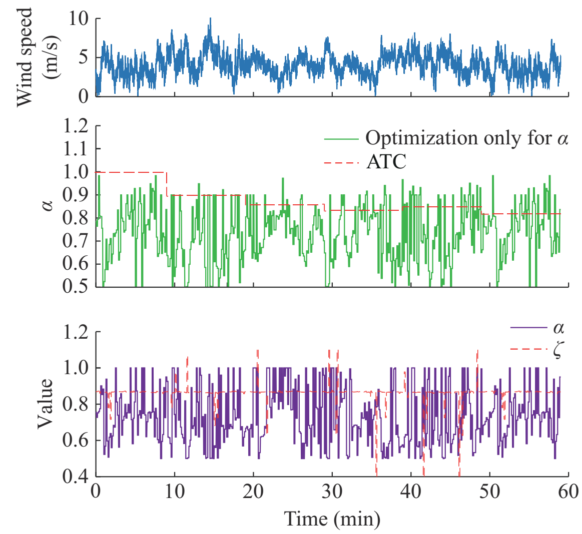

Fig. 11. Comparison of α for different methods using FAST simulation.

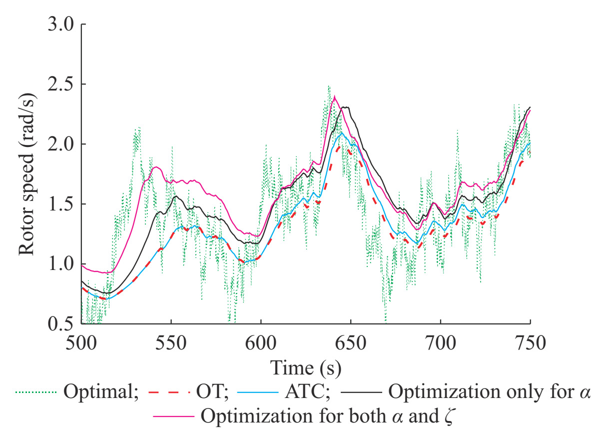

Fig. 12. Comparison of rotor speeds for different methods using FAST simulation.

As shown in Table II, the wind energy extraction efficiency with the proposed method is enhanced compared with that of the ATC method. Furthermore, the optimal command with α^* and ζ^* results in larger efficiency than that with α^*. It means that a higher degree of freedom of the power curve adjustment can improve the optimization effect. The rotor accelerates by tending toward the maximum energy capture, although an accurate wind signal is not obtained with the persistence method for a prediction time window.

TABLE II
COMPARISON OF WIND ENERGY EXTRACTION EFFICIENCY USING FAST SIMULATION

Method	η (%)
OT	85.10
ATC	88.02
Optimal command with α^*	89.83
Optimal command with α^* and ζ^*	92.13

The efficiency of wind energy capture is calculated using (8). Compared with ATC, the proposed method in this paper is better adapted to varying wind speeds, thereby capturing more energy.

However, in this method, the optimization effect of wind energy efficiency is greatly affected by the selection of the ranges of the prediction and control time windows. An inappropriate v_{ξ} may lead to a decrease in wind energy extraction. A better technique for wind speed forecasting may obtain a better effect.

B. Experimental Validation

To verify the proposed method, a WTS-based wind turbine generator (WTG) test bench [33] that can replicate the mechanical dynamics of the CART3 turbine is established. As shown in Fig. 13(b), the test bench includes three main parts, i.e., WTS, electrical part and Beckhoff PLC.

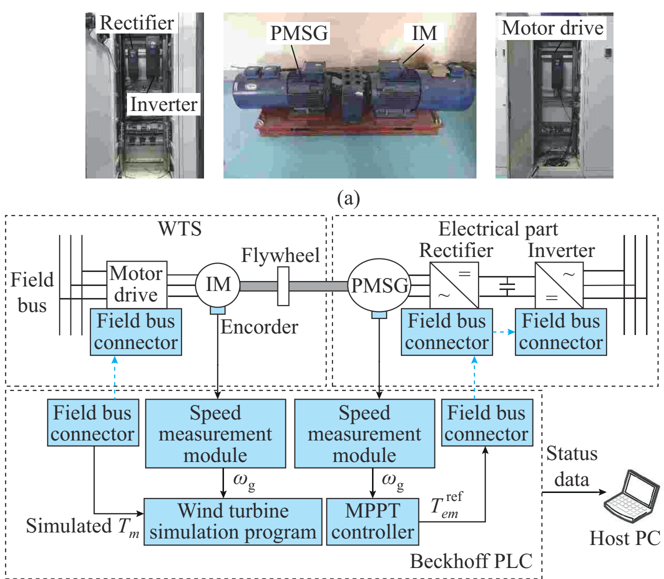

Fig. 13. WTS-based WTG test bench. (a) Laboratory implementation for experimental testing. (b) Schematic diagram of WTS-based WTG test bench.

The WTS consists of an induction motor (IM), a flywheel, and a simulation program running on a programmable logic controller (PLC). The aeroelastic simulation program is developed by FAST code, mainly containing the aerodynamic simulation algorithm and the rotor inertia compensation algorithm. By combining the simulation program and the deployment of the flywheel [33], the aerodynamic behavior and the mechanical dynamics of the CART3 turbine can be simulated by the WTS.

The electrical part includes a permanent-magnet synchronous generator (PMSG) and a grid-connected convertor (including a generator-side rectifier coupled with a grid-side inverter). These parts are implemented in the practical WTG. The rectifier controls the PMSG torque through the torque reference received from the Beckhoff PLC.

The MPPT control algorithms implemented on the PLC send the electromagnetic torque reference to the rectifier at each control cycle.

The comparison of different MPPT methods with the same wind profile input and parameter settings noted in Section IV-A are implemented through the test bench. As shown in Figs. 14-16 and Table III, the experimental results, similar to those of the FAST simulation, further demonstrate the merits of the proposed method. During these experiments, the following points are noted.

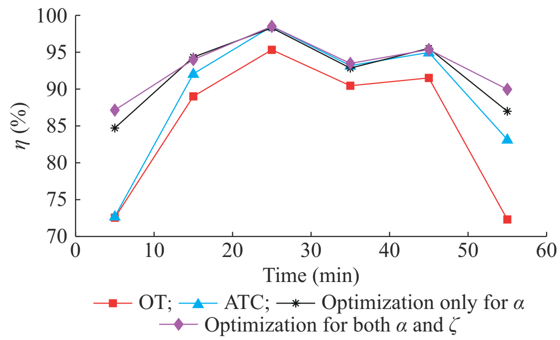

Fig. 14. Comparison of η for different methods in experimental validation.

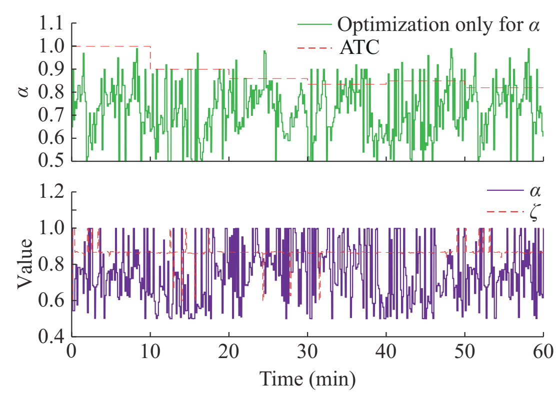

Fig. 15. Comparison of α for different methods in experimental validation.

1) The optimization of α proposed in this paper better adapts to varying wind speeds. This thereby improves the wind energy extraction efficiency even further.

2) Although the effect of the factor ζ is similar to that of α on the dynamic performance, the wind energy extraction efficiency is further enhanced. The fluctuation of the factor ζ matched dynamically is approximately constant compared with the varying α.

3) The rotor speed trajectories in the experimental results produce few jagged fluctuations due to the measured noise compared with the simulation results.

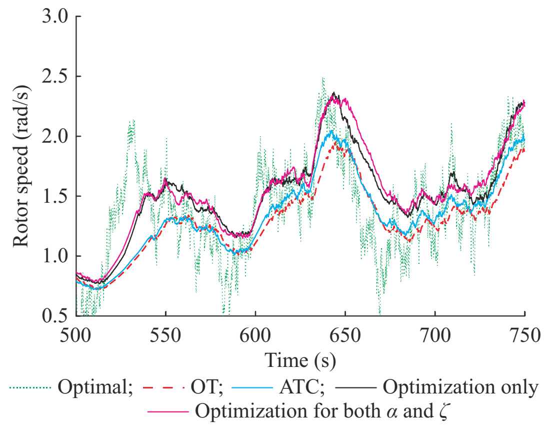

Fig. 16. Comparison of rotor speeds for different methods in experimental validation.

TABLE III
COMPARISON OF WIND ENERGY EXTRACTION EFFICIENCY IN EXPERIMENTAL VALIDATION

Method	η (%)
OT	86.91
ATC	90.55
Optimal command with α^*	92.84
Optimal command with α^* and ζ^*	93.55

V. CONCLUSION

From the perspective of the power losses incurred when tracking rapidly changing wind speeds, this paper provides a feasible and efficient method to optimize the power curve modification factors in shorter cycles.

Considering that the modification factor update cycles utilized in previously developed OT control methods are too long to adapt to varying wind speeds, this paper optimizes the modification factors corresponding to the maximum prospective extracted wind energy. To overcome the challenge of computing optimal solutions to real-time wind turbine control problems, offline mapping can be established based on wind speed forecasting through the persistence method. In this way, the generated torque command is updated and periodically mapped through the online estimated wind speed and measured rotor speed. Simulation and experimental results verify that the proposed method improves the wind energy extraction efficiency.

APPENDIX A

To ensure the stability of a wind turbine with controller (13), the following theorem is given.

Theorem 1: suppose that the input wind speed v is constant. Then, the equilibrium point $\omega_r=\omega_e$ of plant (6) and controller (13) is locally asymptotically stable.

Proof: let

$$h(\lambda)=\frac{\alpha K_{opt} v^2 \lambda^3-\zeta R^2 \lambda}{\frac{1}{2}\rho\pi R^5 v^2} \tag{A1}$$

In Fig. A1, the graphs of functions $C_p(\lambda)$ and $h(\lambda)$ are plotted using the parameters in Table I. The abscissa of the intersection of the two curves is defined as λ_e at a rotor speed ω_e.

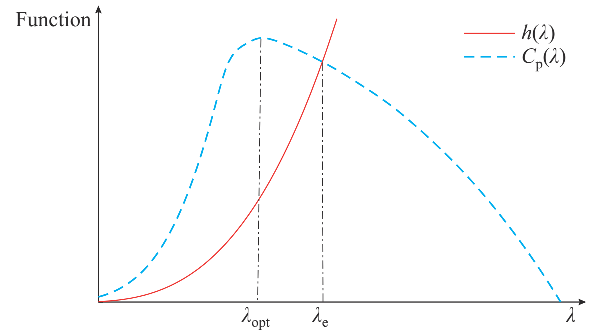

Fig. A1. Functions of $C_p(\lambda)$ and $h(\lambda)$.

Suppose that $V(x)=\frac{1}{2}e^2$ is a Lyapunov function, where $e=\omega-\omega_e$. Then,

$$\begin{aligned}\dot{V}(\omega)&=e\dot{e}=(\omega-\omega_e)\dot{\omega}=\\ &\frac{v}{R}(\lambda-\lambda_e)\left(\frac{1}{2}\rho\pi R^3 v^2\frac{C_p(\lambda)}{\lambda}-\alpha K_{opt}\omega^2+\zeta\right)\\ &\frac{2\lambda}{\rho\pi R^4 v}(\lambda-\lambda_e)(C_p(\lambda)-h(\lambda))<0\end{aligned} \tag{A2}$$

Therefore, the wind power system (1)-(6) at the equilibrium point $\omega=\omega_e$ is asymptotically stable.

The rotor speed converges to a certain state. Note that the prototype of the constructor in (A1) can be found in [8].

APPENDIX B

More details are provided regarding the solution of the objective function in (14) and (15). To solve (15), an optimal control model is transformed by the wind turbine model with DTG control. The standard optimal control formulation is summarized as follows.

1) The performance index is the maximum level of wind energy extraction in the time interval $[0,\tau]$:

$$obj=0.5\rho\pi R^2\int_0^\tau v(t)^3(C_p^{\max}-C_p(\lambda))\mathrm{d}t \tag{B1}$$

2) The state equation is the equation of motion, in which the rotor speed ω_r is the system statement:

$$\dot{\omega}_r=(T_r-T_g)/J_t \tag{B2}$$

3) The control variable is the modification factor due to the fixed form of the electromagnetic torque command, as shown in (B3), which meets the constraints of (16).

$$\boldsymbol{u}=(\alpha,\zeta)^T \tag{B3}$$

4) The initial status $\omega_r(0)$ is the measured value in each control cycle.

From the Pontryagin maximum principle, it follows that the necessary condition for the globally optimal solution to the optimal control problem 1)-4) is given by:

$$H(\omega_r^*,p,u^*,t)=\min H(\omega_r^*,p,u,t) \tag{B4}$$

where ω_r^* is the optimal state variable; u^* is the optimal control variable; p is the costate variable; and H is the Hamiltonian function defined as:

$$H = 0.5\rho\pi R^2 v^3 (C_p^{\max} - C_p(\lambda)) + p^{\tau}(T_r - T_g)/J_t \tag{B5}$$

Usually, it is difficult to obtain an analytical u^* value from (B4). In this paper, the Gaussian pseudospectral method is applied to solve the optimal control problem numerically. Due to the superiority of the Gaussian pseudospectral method, related software based on this method has also been developed. A MATLAB software program called GPOPS-II, which uses a variable-order Gaussian integral pseudospectral method to solve the general continuous-time optimal control problem, is used to compute the solution of the optimal control problem in this paper.

In GPOPS-II, three main files corresponding to the performance index, state equation, and constraints are written first. In these files, the variables are defined in the programming language of GPOPS-II according to the optimal control problem 1)-4). By running the program, the optimal u^* can be obtained.

References

[1] J. Albuquerque, R. Aquino, O. Neto *et al.*, "Power curve modelling for wind turbine using artificial intelligence tools and pre-established inference criteria," *Journal of Modern Power Systems and Clean Energy*, vol. 9, no. 3, pp. 526-533, Oct. 2020.

[2] D. Zouheyr, B. Lotfi, and B. Abdelmadjid, "Improved hardware implementation of a TSR based MPPT algorithm for a low cost connected wind turbine emulator under unbalanced wind speeds," *Energy*, vol. 232, p. 121039, Oct. 2021.

[3] M. M. Ahmed, W. S. Hassanein, N. A. Elsonbaty *et al.*, "Proposing and evaluation of MPPT algorithms for high-performance stabilized WIND turbine driven DFIG," *Alexandria Engineering Journal*, vol. 59, no. 6, pp. 5135-5146, Dec. 2020.

[4] D. Bustan and H. Moodi, "Adaptive interval type-2 fuzzy controller for variable-speed wind turbine," *Journal of Modern Power Systems and Clean Energy*, vol. 10, no. 2, pp. 524-530, Mar. 2022.

[5] K. Johnson, L. Fingersh, M. Balas *et al.*, "Methods for increasing region 2 power capture on a variable-speed wind turbine," *Journal of Solar Energy Engineering*, vol. 126, no. 4, pp. 1092-1100, Nov. 2004.

[6] M. Hand, K. Johnson, L. Fingersh *et al.* (2004, May). Advanced control design and field testing for wind turbines at the National Renewable Energy Laboratory. [Online]. Available: http://www.nrel.gov/docs/fy04osti/36118.pdf

[7] T. Burton, D. Sharpe, N. Jenkins *et al.*, *Wind Energy Handbook*. New York: Wiley, 2001, pp. 475-523.

[8] K. Johnson, L. Pao, M. Balas *et al.*, "Control of variable-speed wind turbines: standard and adaptive techniques for maximizing energy capture," *IEEE Control Systems Magazine*, vol. 26, no. 3, pp. 70-81, Jul. 2006.

[9] K. Johnson. (2004, Aug.). Adaptive torque control of variable speed wind turbines. [Online]. Available: http://nrel.gov/docs/fy04osti/36265.pdf

[10] X. Zhang, C. Huang, S. Hao *et al.*, "An improved adaptive-torque-gain MPPT control for direct-driven PMSG wind turbines considering wind farm turbulences," *Energies*, vol. 9, no. 11, p. 977, Nov. 2016.

[11] X. Zhang, Y. Zhang, S. Hao *et al.*, "An improved maximum power point tracking method based on decreasing torque gain for large scale wind turbines at low wind sites," *Electric Power Systems Research*, vol. 176, p. 105942, Nov. 2019.

[12] K. H. Kim, T. L. Van, D. C. Lee *et al.*, "Maximum output power tracking control in variable-speed wind turbine systems considering rotor inertial power," *IEEE Transactions on Industrial Electronics*, vol. 60, no. 8, pp. 3207-3217, Aug. 2013.

[13] J. Chen, J. Chen, and C. Gong, "Constant-bandwidth maximum power point tracking strategy for variable-speed wind turbines and its design details," *IEEE Transactions on Industrial Electronics*, vol. 60, no. 11, pp. 5050-5059, Nov. 2013.

[14] M. Yin, X. Zhang, X. Ye *et al.*, "Improved MPPT control based on the reduction of tracking range," *Proceedings of the CSEE*, vol. 32, no. 27, pp. 24-31, Sept. 2012.

[15] M. Yin, X. Zhang, Y. Zou *et al.*, "Improved MPPT control of wind turbines based on optimization of tracking range," *Power System Technology*, vol. 38, no. 8, pp. 2180-2185, Aug. 2014.

[16] M. Yin, W. Li, C. Chung *et al.*, "Optimal torque control based on effective tracking range for maximum power point tracking of wind turbines under varying wind conditions," *IET Renewable Power Generation*, vol. 11, no. 4, pp. 501-510, Nov. 2016.

[17] X. Ye, M. Yin, X. Zhang *et al.*, "Convergence problem of adaptive torque control used in wind power generation system," *Energies*, vol. 9, no. 11, pp. 1-16, Jan. 2016.

[18] S. Dickler, M. Wiens, F. Thonnissen *et al.*, "Requirements on super-short-term wind speed predictions for model predictive wind turbine control," in *Proceedings of 2019 IEEE European Control Conference*, Naples, Italy, Jan. 2019, pp. 3346-3352.

[19] Z. Tian and H. Chen, "Multi-step short-term wind speed prediction based on integrated multi-model fusion," *Applied Energy*, vol. 298, p. 117248, Sept. 2021.

[20] Y. Zhou, Y. Sun, S. Wang *et al.*, "Performance improvement of very short-term prediction intervals for regional wind power based on composite conditional nonlinear quantile regression," *Journal of Modern Power Systems and Clean Energy*, vol. 10, no. 1, pp. 60-70, Jan. 2022.

[21] H. Liu, Z. Duan, and C. Chen, "Wind speed big data forecasting using time-variant multi-resolution ensemble model with clustering auto-encoder," *Applied Energy*, vol. 280, no. 15, p. 115975, Dec. 2020.

[22] A. Costa, A. Crespo, J. Navarro *et al.*, "A review on the young history of the wind power short-term prediction," *Renewable and Sustainable Energy Reviews*, vol. 12, no. 6, pp. 1725-1744, Aug. 2008.

[23] J. M. Jonkman and J. M. Buhl. (2005, Aug.). FAST user's guide. [Online]. Available: http://www.nrel.gov/docs/fy06osti/38230.pdf

[24] M . Yin, W. Li, C. Chung *et al.*, "Inertia compensation scheme of WTS considering time delay for emulating large-inertia turbines," *IET Renewable Power Generation*, vol. 11, no. 4, pp. 529-538, Mar. 2017.

[25] C. T. Pan and Y. L. Juan, "A novel sensorless MPPT controller for a high-efficiency microscale wind power generation system," *IEEE Transactions on Energy Conversion*, vol. 25, no. 1, pp. 207-216, Mar. 2010.

[26] Y. Zhang, G. Pan, B. Chen *et al.*, "Short-term wind speed prediction model based on GA-ANN improved by VMD," *Renewable Energy*, vol. 156, pp. 1373-1388, Aug. 2020.

[27] Y. Dong, S. Ma, H. Zhang *et al.*, "Wind power prediction based on multi-class autoregressive moving average model with logistic function," *Journal of Modern Power Systems and Clean Energy*, vol. 10, no. 5, pp. 1184-1193, Sept. 2022.

[28] B. Boukhezzar and H. Siguerdidjane, "Nonlinear control of a variable-speed wind turbine using a two-mass model," *IEEE Transactions on Energy Conversion*, vol. 26, no. 1, pp. 149-162, Mar. 2011.

[29] Z. Chen, M. Yin, L. Zhou *et al.*, "Variable parameter nonlinear control for maximum power point tracking considering mitigation of drive-train load," *IEEE/CAA Journal of Automatica Sinica*, vol. 4, no. 2, pp. 252-259, Apr. 2017.

[30] M. Patterson and A. Rao, "GPOPS-II: a MATLAB software for solving multiple-phase optimal control problems using *hp*-adaptive Gaussian quadrature collocation methods and sparse nonlinear programming," *ACM Transactions on Mathematical Software*, vol. 41, no. 1, pp. 1-37, Oct. 2014.

[31] C. M. Digirolamo, "Applications of GPOPS-II to optimal control problems with delays," Ph. D. dissertation, Department of Mathematics, North Carolina State University, Raleigh, USA, 2020.

[32] J. Betts, S. Campbell, and C. Digirolamo, "Examination of solving optimal control problems with delays using GPOPS-II," *Numerical Algebra, Control and Optimization*, vol. 11, no. 2, pp. 283-305, Jun. 2021.

[33] J. Y. Park, J. K. Lee, K. Y. Oh *et al.*, "Design of simulator for 3 MW wind turbine and its condition monitoring system," in *Proceedings of 2010 International MultiConference of Engineers Computer Scientists*, Hong Kong, China, Mar. 2010, pp. 930-933.

Liansong Guo received the B.S. degree in 2018 in mathematics from Nanjing University of Science and Technology, Nanjing, China, where he is currently working toward the Ph.D. degree in control science and engineering with the School of Automation. His research interest includes wind turbine control.

Minghui Yin received the B.Eng. and M.Eng. degrees in electrical power engineering, and the Ph.D. degree in control science and engineering from Nanjing University of Science and Technology, Nanjing, China, in 1999, 2002, and 2009, respectively. From July 2007 to July 2008, he was a Research Assistant with the Department of Electrical Engineering, The Hong Kong Polytechnic University, Hong Kong, China. From January 2016 to January 2017, he was a Visiting Scholar with the School of Electrical and Information Engineering, the University of Sydney, Sydney, Australia. He is currently a Professor with the School of Automation, Nanjing University of Science and Technology. His main research interests include wind power conversion system and power system transient stability.

Chenxiao Cai received the Ph.D. degree in control science and engineering from Nanjing University of Science and Technology, Nanjing, China, in 2005. She is currently a Professor with the School of Automation, Nanjing University of Science and Technology. Her main research interests include singularly perturbed systems, singular systems, robust control, unmanned aerial vehicle, and deep learning algorithm.

Yunyun Xie received the B.Eng. degree in electrical power engineering and the Ph.D. degree in control science and engineering from Nanjing University of Science and Technology, Nanjing, China, in 2007 and 2013, respectively. He is currently an Assistant Professor with the School of Automation, Nanjing University of Science and Technology. His main research interests include power system restoration and power system transient stability.

Yun Zou received the B.S. degree in mathematics from Northwestern University, Xi'an, China, in 1983, and the M.S. and Ph.D. degrees in control theory and control engineering from Nanjing University of Science and Technology, Nanjing, China, in 1987 and 1990, respectively. He is currently a Professor with the School of Automation, Nanjing University of Science and Technology. His current research interests include differential-algebraic equation systems, two-dimensional systems, singular perturbations, transient stability of power systems, and electricity market.